Article

Synthesis, Crystallization Mechanism, and Catalytic Properties of Titanium-Rich TS-1 Free of Extraframework Titanium Species

Weibin Fan, Ren-Guan Duan, Toshiyuki Yokoi, Peng Wu, Yoshihiro Kubota, and Takashi Tatsumi

J. Am. Chem. Soc., **2008**, 130 (31), 10150-10164 • DOI: 10.1021/ja7100399 • Publication Date (Web): 10 July 2008

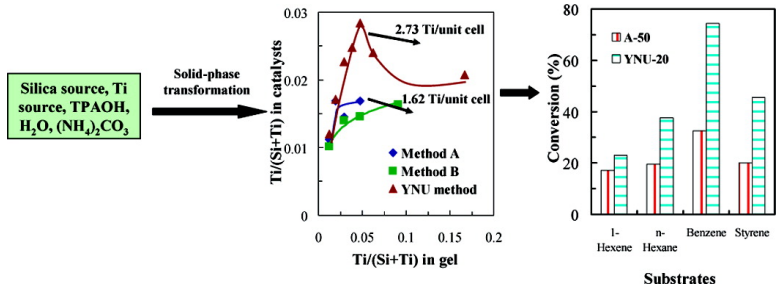

More About This Article

Additional resources and features associated with this article are available within the HTML version:

- Supporting Information
- Access to high resolution figures
- Links to articles and content related to this article
- Copyright permission to reproduce figures and/or text from this article

View the Full Text HTML

J|A|C|S
ARTICLES

Published on Web 07/10/2008

Synthesis, Crystallization Mechanism, and Catalytic Properties of Titanium-Rich TS-1 Free of Extraframework Titanium Species

Weibin Fan,[†,‡] Ren-Guan Duan,[§] Toshiyuki Yokoi,[†] Peng Wu,[||] Yoshihiro Kubota,[⊥] and Takashi Tatsumi*[,†]

Catalytic Chemistry Division, Chemical Resources Laboratory, Tokyo Institute of Technology, Nagatsuta 4259, Midori-ku, Yokohama 226-8503, Japan, State Key Laboratory of Coal Conversion, Institute of Coal Chemistry, Chinese Academy of Sciences, 27 South Taoyuan Road, Taiyuan 030001, China, Mail Stop D469, EES-6, Los Alamos National Laboratory, Los Alamos, New Mexico 87545, Shanghai Key Laboratory of Green Chemistry and Chemical Processes, Department of Chemistry, East China Normal University, North Zhongshan Road 3663, Shanghai 200062, China, and Catalysis Laboratory, Division of Materials Science and Chemical Engineering, Faculty of Engineering, Yokohama National University, Tokiwadai 79-5, Hodogaya-ku, Yokohama 240-8501, Japan

Received November 14, 2007; E-mail: ttatsumi@cat.res.titech.ac.jp

Abstract: A new route to the synthesis of TS-1 has been developed using $(NH_4)_2CO_3$ as a crystallization-mediating agent. In this way, the framework Ti content can be significantly increased without forming extraframework Ti species. The prepared catalyst had a Si/Ti ratio as low as 34 in contrast to the ratio of 58 achieved with the methods **A** and **B** established by the Enichem group (Clerici, M. G.; Bellussi, G.; Romano, U. *J. Catal.* 1991, 129, 159) and Thangaraj and Sivasanker (Thangaraj, A.; Sivasanker, S. *J. Chem. Soc., Chem. Commun.* 1992, 123), respectively. The material contained less defect sites than the samples synthesized by the other two methods. As a result, it showed much higher activity for the oxidation of various organic substrates, such as linear alkanes/alkenes and alcohols, styrene, and benzene. The crystallization mechanism of TS-1 in the presence of $(NH_4)_2CO_3$ was studied by following the whole crystallization process with X-ray diffraction (XRD), field emission scanning electron microscopy (FE-SEM), thermogravimetry/differential thermal analysis (TG/DTA), inductively coupled plasma atomic emission spectrometry (ICP), Fourier transform infrared spectroscopy (FTIR), X-ray photoelectron spectroscopy (XPS), diffuse reflectance UV−vis spectroscopy, and ^{29}Si MAS (magic-angle spinning) NMR spectroscopy techniques. It was shown that the presence of $(NH_4)_2CO_3$ not only drastically lowered down pH, slowing down the crystallization process and making the incorporation of Ti into the framework match well with nucleation and crystal growth, but also modified the crystallization mechanism. It seems that the solid-phase transformation mechanism predominated in the crystallization process initiated by dissociation, reorganization, and recoalescence of the solidified gel although a small amount of nongelatinated Ti shifted to the solid during the crystal growth period. In contrast, a typical homogeneous nucleation mechanism occurred in the method **A** system. Thus, although in the method **A** system most of Ti cations was inserted into the lattice after the crystallization was nearly completed, the inclusion of Ti started at the earlier nucleation period in the presence of $(NH_4)_2CO_3$. This is favorable for the incorporation of Ti into the framework, resulting in a more homogeneous distribution of Ti in the framework. Oxidation of 1-hexene and 2-hexanol over the samples collected during the whole crystallization process indicated that condensation of Ti−OH and Si−OH proceeded even after the crystallization was completed. This resulted in an increase in hydrophobicity and an overall improvement in microscopic character of Ti species and consequently a great increase in the catalytic activity with further progress of crystallization.

1. Introduction

The discovery of TS-1 is a milestone in zeolite and heterogeneous catalysis research fields. This is because it is an active, highly selective, and environmentally benign catalyst for a number of industrially important organic oxidation reactions in the presence of aqueous H_2O_2 solution. Typical reactions include the conversion of alkanes to alcohols and ketones, secondary alcohols to ketones, secondary amines and ammonia to dialkylhydroxylamines and hydroxylamine, as well as alkene epoxidation, phenol oxidation, ketone ammoximation, etc.[1–7]

[†] Tokyo Institute of Technology.
[‡] Institute of Coal Chemistry, Chinese Academy of Sciences.
[§] Los Alamos National Laboratory.
[||] East China Normal University.
[⊥] Yokohama National University.

(1) Tatsumi, T.; Nakamura, M.; Negishi, S.; Tominaga, H. *Chem. Commun.* **1990**, 476.
(2) Notari, B. *Adv. Catal.* **1996**, *41*, 253, and references therein.

10.1021/ja7100399 CCC: $40.75

The catalytic property of TS-1 depends on the lattice Ti content, which is, however, usually less than 2 wt %.[8,9] The effective way to increase the Ti content in the framework of TS-1 is still a huge challenge. Thangaraj and Sivasanker reported that eight Ti ions could be incorporated in the lattice sites per unit cell by an improved method (method **B**) in which titanium tetra-*n*-butoxide was first dissolved in isopropyl alcohol before addition to the hydrolyzed tetraethyl orthosilicate aqueous solution for the purpose of avoiding formation of TiO_2 precipitate by reducing the hydrolysis rate of the alkoxide,[10] but Schuchardt et al. could not reproduce it, and found that there was no difference in the framework Ti content between the samples synthesized by methods **A** and **B**.[11] This is also proven by our data shown in the following section.

To synthesize Ti-rich TS-1, it is necessary and helpful to make its crystallization mechanism clear. However, very few reports have been devoted to the study of this subject.[12] This might be due to the complexity of the zeolite crystallization mechanism. Indeed, it involves both nucleation and crystal growth,[12–27] and both have numerous simultaneous and independent equilibria and condensation steps while nanoaggregates might evolve into zeolite crystals.[17–27] In addition, the synthesis materials, i.e., silica source, solvent, and templating/structure-directing agent as well as the crystallization promoter or inhibitor, also significantly affect the crystallization mechanism. As a result, with respect to nucleation, there are several models, including homogeneous nucleation, heterogeneous nucleation, autocatalytic nucleation, and secondary nucleation, and different nucleation processes have been tried to be accounted for by different models.[12,13,17–27] In the case of crystallization growth, a transition period involving a slow growth of a crystalline phase and a relatively rapid crystal growth period are included. Crystallization in hydrothermal systems may occur through the liquid-phase transformation mechanisms,[13–27] whereas in nonaqueous systems the crystallization mechanism via solid-phase transformation seems to predominate.[13,14] In contrast, in the case of synthesis of ZSM-5 in the system free of solvent by using TPABr and NH_4F as cotemplates, a vapor phase transport mechanism has been suggested.[28] Therefore, up to date, although more than 170 types of zeolitic materials with various uniform topologies have been synthesized and some of them have been widely used in petrochemical and fine chemical industries as active and selective catalysts and/or effective adsorbents, their crystallization mechanisms have not been clear yet. A full understanding of the crystallization mechanisms is desirable for the synthesis of conventional zeolites with significantly improved performance and new zeolites.

The crystallization process of titanosilicates is much more complex than that of aluminosilicates because Ti^{4+} has a weak structure-directing role and is much more difficult to be incorporated into the framework than Al^{3+}. As we know, isomorphous substitution of metal atoms for Si in zeolites is not only related to zeolite structures/framework composition flexibility and the chemical nature of metals[29–33] but is also strongly influenced by the crystallization mechanism. The framework composition flexibility of zeolites is chemically important. Isomorphous substitution of transition metal ions for Si requires a flexibility of the framework to bring together a cluster of oxygen atoms around metal cations.[32] This could be made easier by hosting many defect sites in the framework.[9,34,35] Therefore, the more flexible the framework of zeolites is, the higher the substitution degree is.[33] Thus, more Ti species could be incorporated into the framework of Ti-Beta and Ti-MWW than into that of TS-1.[36,37] Nevertheless, Ti K edge extended X-ray absorption fine structure (EXAFS) studies have shown that the Ti−O bond length of tetrahedral $Ti(OSi)_4$ species is about 1.80 Å in contrast to the 1.61 Å of the Si−O bond length.[35,38–43] The Ti−O bond is much longer than the Si−O bond, probably making the local structure around Ti seriously

(3) Clerici, M. G.; Ingallina, P. *J. Catal.* **1993**, *140*, 71.
(4) Bellussi, G.; Rigutto, M. S. *Stud. Surf. Sci. Catal.* **1994**, *85*, 177.
(5) Ratnasamy, P.; Srinivas, D.; Knözinger, H. *Adv. Catal.* **2004**, *48*, 1.
(6) Bhaumik, A.; Kumar, R. *J. Chem. Soc., Chem. Commun.* **1995**, 349.
(7) Bhaumik, A.; Samanta, S.; Mal, N. M. *Microporous Mesoporous Mater.* **2004**, *68*, 29.
(8) Bordiga, S.; Damin, A.; Bonino, F.; Ricchiardi, G.; Zecchina, A.; Tagliapietra, R.; Lamberti, C. *Phys. Chem. Chem. Phys.* **2003**, *5*, 4390.
(9) Lamberti, C.; Bordiga, S.; Zecchina, A.; Artioli, G.; Marra, G.; Spano, G. *J. Am. Chem. Soc.* **2001**, *123*, 2204.
(10) Thangaraj, A.; Sivasanker, S. *J. Chem. Soc., Chem. Commun.* **1992**, 123.
(11) Schuchardt, U.; Pastore, H. O.; Spinace, E. V. *Stud. Surf. Sci. Catal.* **1994**, *84*, 1877.
(12) Serrano, D. P.; Uguina, M. A.; Ovejero, G.; van Grieken, R.; Camacho, M. *Microporous Mater.* **1996**, *7*, 309.
(13) Fan, W.; Li, R.; Ma, J.; Fan, B.; Dou, T.; Cao, J. *Microporous Mater.* **1997**, *8*, 131.
(14) Xu, R.; Tu, K.; Pang, W. *Zeolite Molecular Sieves Structure and Synthesis*; Jilin University Publisher, 1987.
(15) Burkett, S. L.; Davis, M. E. *J. Phys. Chem.* **1994**, *98*, 4647.
(16) Burkett, S. L.; Davis, M. E. *Chem. Mater.* **1995**, *7*, 920.
(17) Dokter, W. H.; van Garderen, H. F.; Beelen, T. P. M.; van Santen, R. A.; Bras, W. *Angew. Chem., Int. Ed. Engl.* **1995**, *34*, 73.
(18) Mintova, S.; Olson, N. H.; Valtchev, V.; Bein, T. *Science* **1999**, *283*, 958.
(19) Mintova, S.; Olson, N. H.; Bein, T. *Angew. Chem., Int. Ed.* **1999**, *38*, 3201.
(20) Davis, T. M.; Drews, T. O.; Ramanan, H.; He, C.; Dong, J.; Schnablegger, H.; Katsoulakis, M. A.; Kokkoli, E.; Mccormick, A. V.; Penn, R. L.; Tsapatsis, M. *Nat. Mater.* **2006**, *5*, 400.
(21) Ravishankar, R.; Kirschhock, C. E. A.; Knops-Gerritis, P. P.; Feijen, E. J. P.; Grobet, P. J.; Vanoppen, P.; De Schryver, F. C.; Miehe, G.; Fuess, H.; Schoeman, B. J.; Jacobs, P. A.; Martens, J. A. *J. Phys. Chem. B* **1999**, *103*, 4960.
(22) Kirschhock, C. E. A.; Ravishankar, R.; Verspeurt, F.; Grobet, P. J.; Jacobs, P. A.; Martens, J. A. *J. Phys. Chem. B* **1999**, *103*, 4965.
(23) Kirschhock, C. E. A.; Ravishankar, R.; van Looveren, L.; Jacobs, P. A.; Martens, J. A. *J. Phys. Chem. B* **1999**, *103*, 4972.
(24) Kirschhock, C. E. A.; Buschmann, V.; Kremer, S.; Ravishankar, R.; Houssin, C. J. Y.; Mojet, B. L.; van Santen, R. A.; Grobet, P. J.; Jacobs, P. A.; Martens, J. A. *Angew. Chem., Int. Ed.* **2001**, *40*, 2637.
(25) Kirschhock, C. E. A.; Kremer, S. P. B.; Grobet, P. J.; Jacobs, P. A.; Martens, J. A. *J. Phys. Chem. B* **2002**, *106*, 4899.
(26) De Moor, P. E. A.; Beelen, T. P.; van Santen, R. A. *J. Phys. Chem. B* **1999**, *103*, 1639.
(27) Kirschhock, C. E. A.; Ravishankar, R.; Jacobs, P. A.; Martens, J. A. *J. Phys. Chem. B* **1999**, *103*, 11021.
(28) Althoff, R.; Unger, K.; Schüth, F. *Microporous Mater.* **1994**, *2*, 557.
(29) Fan, W.; Schoonheydt, R. A.; Weckhuysen, B. M. *Chem. Commun.* **2000**, 2249.
(30) Weckhuysen, B. M.; Rao, R. R.; Martens, J. A.; Schoonheydt, R. A. *Eur. J. Inorg. Chem.* **1999**, 565.
(31) Fan, W.; Fan, B.; Song, M.; Chen, T.; Li, R.; Dou, T.; Tatsumi, T.; Weckhuysen, B. M. *Microporous Mesoporous Mater.* **2006**, *94*, 368.
(32) Hammonds, K. D.; Heine, V.; Dove, M. T. *J. Phys. Chem. B* **1998**, *102*, 1759.
(33) Fan, W.; Li, R.; Dou, T.; Tatsumi, T.; Weckhuysen, B. M. *Microporous Mesoporous Mater.* **2005**, *84*, 116.
(34) Artioli, G.; Lamberti, C.; Marra, G. L. *Acta Crystallogr., Sect. B* **2000**, *56*, 2.
(35) Bordiga, S.; Bonino, F.; Damin, A.; Lamberti, C. *Phys. Chem. Chem. Phys.* **2007**, *9*, 4854.
(36) Corma, A.; Camblor, M. A.; Esteve, P.; Martı´nez, A.; Pérez-Pariente, J. *J. Catal.* **1994**, *145*, 151.
(37) Wu, P.; Tatsumi, T. *Chem. Commun.* **2002**, 1026.
(38) Le Noc, L.; Trong On, D.; Solomykina, S.; Echchahed, B.; Béland, F.; Cartier dit Moulin, C.; Bonneviot, L. *Stud. Surf. Sci. Catal.* **1996**, *101*, 611.
(39) Lamberti, C.; Bordiga, S.; Arduino, D.; Zecchina, A.; Geobaldo, F.; Spanò, G.; Genoni, F.; Petrini, G.; Carati, A.; Villain, F.; Vlaic, G. *J. Phys. Chem. B* **1992**, *102*, 6382.

distorted. This results in the slow inclusion of Ti into the framework, compared to Si ions. If crystallization proceeded too fast, Ti ions would not have enough time to be incorporated into the lattice. However, too slow crystallization would possibly cause the formation of transition metal oxides, preventing metal cations from being incorporated into the framework. In addition, the difficult crystallization may also result from the strong competition between the interaction of soluble silicate ions and mother liquor and the condensation of silicate ions. Third, a mismatch among hydrolysis of Ti and Si alkoxides, polymerization of Ti^{4+} and/or Si^{4+} ions, nucleation, and crystal growth would lead to much difficulty in the inclusion of Ti in the framework. Since the chemical nature of Ti and the rigidity of the framework of TS-1 cannot be altered, to find an effective crystallization-mediating agent would be the sole way to increase the lattice Ti content in TS-1 by harmonizing the hydrolysis rate of Ti alkoxide with that of silicate species as well as the nucleation and crystal growth rates. In this respect, we have found the potential of $(NH_4)_2CO_3$; the presence of $(NH_4)_2CO_3$ in the crystallization gel not only considerably increased the framework Ti content without forming extraframework Ti species but also improved the hydrophobicity of the prepared TS-1 catalyst, consequently showing significantly improved activity for the oxidation of a variety of organic substrates.

2. Experimental Section

2.1. Synthesis of Samples. TS-1 samples were synthesized basically according to the procedures reported by the Enichem group[44] (method **A**) except that $(NH_4)_2CO_3$ was added after removing alcohol. Namely, a certain amount of titanium tetra-*n*-butoxide (TBOT) was first dissolved in an aqueous solution of tetrapropylammonium hydroxide (TPAOH), followed by addition of tetraethyl orthosilicate (TEOS) and stirring for 0.5 h. A H_2O_2 aqueous solution (31%) with the mass amount being 3 times as much as that of TBOT was added before the addition of TPAOH. Then, the solution was heated in a water bath kept at 55−60 °C for about 4 h. Occasionally, a small amount of water was added during the heating process to compensate for the vaporized portion. After totally evaporating the alcohol, the resulting clear solution was cooled down, and ammonium carbonate was added. The composition of the final gel was maintained in the range of $0.3(NH_4)_2CO_3/SiO_2/(0-0.2)TiO_2/0.5TPAOH/35H_2O$. The crystallization was carried out at 170 °C for 3−6 days. The solid product was filtered, washed with distilled water, and dried at 100 °C overnight. After drying, the sample was washed with a 1 mol L^{-1} aqueous solution of HCl (at a liquid-to-solid ratio of 50 mL g^{-1}) for 24 h, followed by calcining at 550 °C for 10 h. The calcined sample was further treated with HCl under the same conditions as those set before calcination. Here, this synthesis system is denoted by the YNU system in contrast to the method **A** system.

The crystallization mechanism was studied by following the crystallization process with several autoclaves (150 mL) filled with the gel prepared from 20.1 g of TEOS, 0.65 g of TBOT (monomer, 97%), 41.8 g of TPAOH (20−25% in aqueous solution), 2.13 g of $(NH_4)_2CO_3$, and 25.9 g of distilled water according to the procedures described in the above paragraph. Usually, the crystallization of MFI-type materials proceeds very quickly at high temperature when TPAOH is used as a templating molecule. Therefore, herein the samples were synthesized at the temperatures of 30, 60, 80, 100, 110, 120, 140, or 170 °C with accuracy of ±2 °C in order to control the process. When the designed time was reached, products were withdrawn from the autoclave and quenched in an ice−water mixture. The solid samples were centrifuged to separate them from the mother liquid. Then, the solid samples were fully washed with deionized water and dried at 100 °C. The dried sample was finally calcined at 550 °C for 10 h and washed with 0.5 M aqueous solution of HCl (at a liquid-to-solid ratio of 50 mL g^{-1}). Part of the mother liquid was diluted with deionized water to 100 times in volume for elemental analyses. The crystallization experiments on the method **A** system were carried out similarly.

2.2. Characterization of Samples. The X-ray diffraction patterns (XRD) were recorded by a MAC Science M3X 1030 X-ray diffractometer with Cu Kα radiation (40 kV, 20 mA) to identify the crystalline phase and estimate the crystallinity of TS-1. The diffuse reflectance (DR) UV−vis spectra were measured on a Jasco V-550 UV−vis spectrophotometer with a $BaSO_4$ plate as the reference. Framework infrared (IR) spectra were acquired on a Perkin-Elmer Spectrum One Fourier transform infrared (FTIR) spectrometer. Before recording the spectra, the samples were evacuated at 500 °C for 2 h under high-vacuum conditions. Field emission scanning electron microscopy (FE-SEM) images were obtained on a Hitachi S-5200 scanning electron microscope. ^{29}Si MAS (magic-angle spinning) NMR measurements were performed on a JEOL JNM-ECA 400 nuclear magnetic resonance spectrometer at ambient temperature. The chemical shift was referred to an external standard of poly(dimethylsilane). The spin rate of the rotor was set at 5.0 KHz. A pulse length of 7 μs with a repetition time of 30 s was applied, and 2000−3000 scans were accumulated. The spectra were deconvoluted with Gaussian−Lorentzian mixed equation. X-ray photoelectron spectra (XPS) were attained on a Shimadzu ESCA 3200 X-ray photoelectron spectrometer with an Mg Kα target. Thermogravimetry/differential thermal analysis (TG/DTA) data were collected by a ULVAC-Riko TGD 9600 thermal analysis system. The chemical compositions of the samples were determined by a Shimadzu ICPS-8000E inductively coupled plasma atomic emission spectrometer (ICP).

2.3. Catalytic Measurements. The liquid-phase oxidation of a variety of organic substrates with H_2O_2 (31% in aqueous solution) was carried out under stirring conditions in a round-bottom flask (20 mL) equipped with a condenser. The temperature was controlled with a water bath. The typical reaction conditions for the oxidation of different organics are given in the footnote of the table and captions of figures. For the oxidation of 1-hexene, 2-hexanol, styrene, and linear *n*-alkanes, the products were analyzed by a Shimadzu GC-14A gas chromatograph equipped with a 50 m OV-1 capillary column and a flame ionization detector. The amount of the unconverted H_2O_2 was determined with a 0.1 M aqueous solution of $Ce(SO_4)_2$ by using a titration method. In the case of benzene oxidation, the product was analyzed by a Shimadzu LC-10AD high-performance liquid chromatograph (HPLC), and the H_2O_2 content was measured by the iodine titration method.

3. Results and Discussion

3.1. Preparation and Characterization of TS-1 Catalysts. The as-synthesized sample showed an XRD pattern typical of the MFI structure, confirming its high purity and crystallinity. Table 1 gives the sample notation of *m*−*n* with *m* and *n* representing the synthesis method and the Si/Ti ratio in the synthesis gel, respectively. It was found that the coordination states of Ti species in the samples were markedly different when different synthesis methods were used; the DR UV−vis spectra showed that there was a considerable amount of octahedral Ti species in the as-synthesized (curve a) and calcined (curve b) **A** (the

(40) Blasco, T.; Camblor, M. A.; Corma, A.; Pŕez-Pariente, J. *J. Am. Chem. Soc.* **1993**, *115*, 11806.
(41) Bordiga, S.; Coluccia, S.; Lamberti, C.; Marchese, L.; Zecchina, A.; Boscherini, F.; Buffa, F.; Genoni, F.; Leofanti, G.; Petrini, G.; Vlaic, G. *J. Phys. Chem.* **1994**, *98*, 4125.
(42) Gleeson, D.; Sankar, G.; Catlow, C. R. A.; Thomas, J. M.; Spanó, G.; Bordiga, S.; Zecchina, A.; Lamberti, C. *Phys. Chem. Chem. Phys.* **2000**, *2*, 4812.
(43) Thomas, J. M.; Sankar, G. *Acc. Chem. Res.* **2001**, *34*, 571.
(44) Clerici, M. G.; Bellussi, G.; Romano, U. *J. Catal.* **1991**, *129*, 159.

Table 1. Catalytic Results of the Prepared TS-1 for the Oxidation of *n*-Hexane[a]

sample	Si/Ti ratio in catalyst	conversion (%) based on *n*-hexane	TON based on H_2O_2	selectivity (%) 2- and 3-ol	selectivity (%) 2- and 3-one	H_2O_2 conversion (%)	H_2O_2 selectivity (%)
A-80	88.5	18.4	119	79.2	20.8	13.2	83.3
A-50	58.3	30.6	140	70.9	29.1	23.3	84.2
A-33	67.6	25.5	136	72.1	27.9	19.6	83.0
A-20	58.3	27.0	125	70.8	29.2	20.2	85.8
B-80	97.5	14.7	108	80.6	19.4	12.1	74.4
B-33	70.3	22.5	127	72.9	27.1	19.4	76.5
B-20	67.4	29.2	161	65.8	34.2	24.3	80.4
B-10	60.0	31.3	166	62.9	37.1	27.9	81.0
YNU-80	82.3	23.6	151	72.8	27.2	17.7	85.5
YNU-50	57.2	36.4	172	65.4	34.6	28.0	86.0
YNU-33	43.0	41.0	161	58.2	41.8	37.1	81.4
YNU-25	39.4	46.4	167	52.9	47.1	41.9	81.2
YNU-20	34.2	50.8	160	52.5	47.6	42.2	89.1
YNU-15	40.6	46.5	173	53.1	46.9	41.8	82.2
YNU-5	47.2	38.3	168	53.7	46.3	34.7	82.0

[a] Reaction conditions: 0.1 g of catalyst, 60 °C, 4 h, 10 mL of CH_3OH as solvent, 10 mmol of *n*-hexane, 20 mmol of H_2O_2 (31% in aqueous solution).

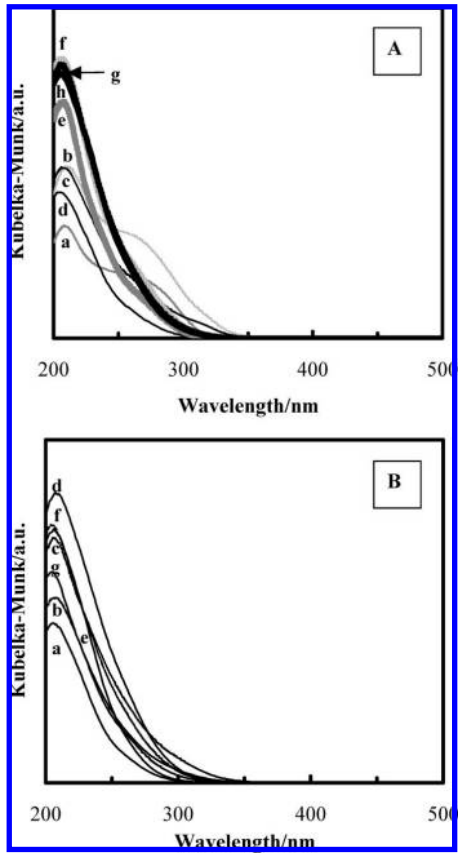

Figure 1. DR UV−vis spectra of (A) TS-1 samples prepared with a synthesis gel having a Si/Ti ratio of 50 by using method **A** (thin lines (a−d)) and the YNU method (thick lines (e−h)). (a and e) as-synthesized, (b and f) calcined, (c and g) calcined and acid-treated, (d and h) acid-treated, calcined, and further acid-washed. (B) DR UV−vis spectra of TS-1 catalysts prepared by the YNU method with a synthesis gel having a Si/Ti ratio of (a) 80, (b) 50, (c) 33, (d) 20, (e) 15, (f) 6.67, and (g) 5.

method **A** employed) samples synthesized from a gel with a Si/Ti ratio of 50, as evidenced by the presence of an intense band around 260 nm in both curves (Figure 1A). In contrast, extraframework octahedral Ti species were negligibly formed in the YNU samples (curves e and f). After acid washing of

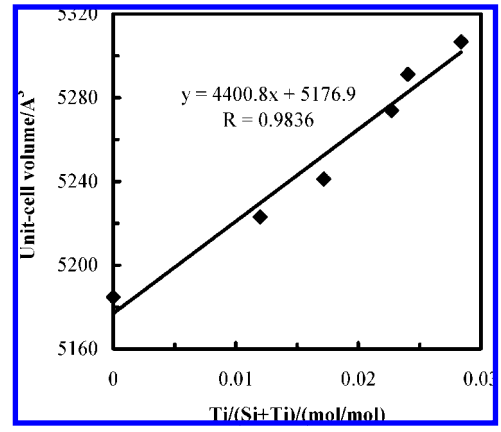

Figure 2. (A) Relationship between the unit-cell volume and Ti content of the TS-1 catalysts prepared from the YNU system (the unit-cell volume was calculated with the Rietveld method by using DBWS software (ref 47)).

calcined samples, a small amount of octahedral Ti species and Ti oxides were still present in the **A** samples (curve c). Nevertheless, if the **A** samples were also treated with acid before calcination, no extraframework Ti species could be detected with the DR UV−vis spectroscopy (curve d). In order to ensure that TS-1 catalysts prepared in the presence of $(NH_4)_2CO_3$ are free of extraframework Ti species, the same acid-treating processes as for the **A** samples were also applied to all the YNU samples.

Table 1 shows that the Si/Ti ratio in the prepared **A** catalysts reached a minimum of 58.3. This corresponds to 1.62 Ti atoms per unit cell. This limitation was further substantiated by progressively increasing the Ti amount in the synthesis gel up to a Si/Ti ratio of 5 (not shown here for brevity). The samples synthesized by method **B** gave similar results. In contrast, if $(NH_4)_2CO_3$ ($(NH_4)_2CO_3/SiO_2$ molar ratio of 0.3) was introduced into the synthesis gel, the Ti content in the catalyst increased with increasing Ti amount in the gel when the Si/Ti ratio in the gel was higher than 20. Attempts to further increase the Ti content in TS-1 by adding more Ti in the synthesis gel as well as by adjusting the amounts of TPAOH and $(NH_4)_2CO_3$ and changing the silica source have been unsuccessful. A decrease in the TPAOH content in the synthesis gel to a TPAOH/Si ratio of 0.42 and 0.35 led to the formation of a TS-1 catalyst with a Si/Ti ratio of 39.1 and 39.6, respectively, when a synthesis gel having a Si/Ti ratio of 20 was used to synthesize TS-1 samples. The use of tetramethyl orthosilicate (TMOS), tetrapropyl orthosilicate (TPOS), fumed silica, and colloidal silica sol, instead of TEOS, as silica sources resulted in the formation of TS-1 catalysts having a Si/Ti ratio in the range of 37−43 under the same synthesis conditions as for the YNU-20 sample. An increase in the $(NH_4)_2CO_3$ content to a $(NH_4)_2CO_3$/Si ratio of 0.5 generated a significant amount of octahedral Ti species, which could not be completely washed away by acid treatment, as confirmed by an intense band at 260 nm in its DR UV−vis spectrum. This also held true for the change of crystallization temperature to 150 or 190 °C.

Figure 2 shows that the unit-cell volume of the TS-1 catalysts prepared from the YNU system linearly increased with increasing Ti content ($V = 4400.8x + 5176.9$, $R = 0.9836$), providing evidence that more Ti cations in the samples have been incorporated into the framework although a systematic decrease in the unit-cell volume was observed compared to the reported values, possibly due to the measurement of the samples under different conditions, the different lattice sites for the inclusion

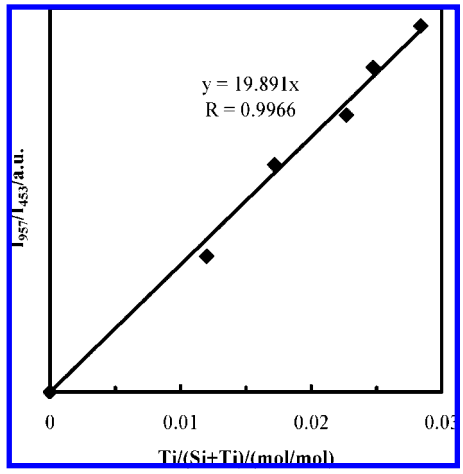

Figure 3. Intensity ratio of the peak at 957 cm^{-1} to that around 453 cm^{-1} as a function of the Ti/(Si + Ti) molar ratio in the TS-1 catalysts prepared by the YNU method.

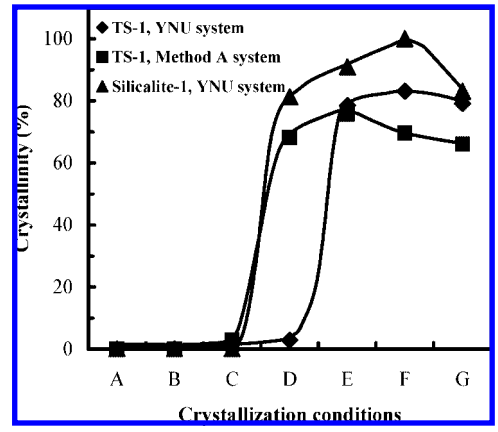

Figure 4. Crystallization curves of TS-1 and silicalite-1 synthesized in the method **A** and YNU systems. (A) 30 °C, 1 day; (B) 60 °C, 1 day; (C) 80 °C, 1 day; (D) 100 °C, 1 day; (E) 140 °C, 1 day; (F) 170 °C, 1 day; (G) 170 °C, 3 days.

of Ti, the increase in the particle size, and the decrease in the defect sites with increasing framework Ti content (to be discussed in detail below), and/or the use of a different refinement program.[45–47] The inclusion of more Ti in the lattice sites with increasing Ti content in the samples is further confirmed by IR spectroscopy. The 960 cm^{-1} band, probably attributed to a stretching vibration mode of [SiO_4] perturbed by an adjacent framework Ti species or of [TiO_4],[48–50] has been widely accepted as a proof of the isomorphous substitution of Ti in the zeolitic lattice. In order to avoid the influence of water and adsorbed molecules on the frequency and intensity of this band,[48] the framework IR spectra of all samples were measured after evacuation at 500 °C under high-vacuum conditions. Figure 3 shows that the absorbance band at about 960 cm^{-1} could not be observed in the IR spectrum of silicalite-1, whereas the intensity of this band in the IR spectra of TS-1 catalysts proportionally increased with increasing Ti amount in the samples ($y = 19.891x$, $R = 0.9966$). The R obtained from the function of (I_{957}/I_{453}) versus (Ti/(Ti + Si)) was larger than that obtained from the function of unit-cell volume versus (Ti/(Ti + Si)), which reveals the considerable effects of the crystal size and the conditions for treating samples on the obtained unit-cell volume. Here, it is worth pointing out that the intensity of the 957 cm^{-1} band was normalized on the basis of the 453 cm^{-1} band, which is assigned to structure-insensitive T−O bending mode of tetrahedral TO_4 units.[19]

DR UV−vis spectroscopy shows only the band at 210 nm, but no band above 250 nm was observed for all the YNU samples synthesized with the gels having different Ti contents (Figure 1B). Although this cannot exclude the possibility of the presence of extraframework Ti species, it definitely verifies that most of the Ti species present in the samples have been incorporated into the framework. This indicates that incorporation of about 2.73 Ti atoms per unit cell could be achieved with the YNU method for sample YNU-20 (Si/Ti = 34.2). This value is much higher than that achieved by methods **A** or **B**. Although some papers reported that the Ti content in the TS-1 could be increased up to a Si/Ti ratio of 40,[46,51] or even of 33,[9,52] substantial difficulty was encountered in the synthesis of well-manufactured samples.[35,46] It requires extremely pure reagents and severe control of the synthesis conditions,[35,46] resulting in a poor reproducibility. This is unlike the YNU method which can use various types of silica sources such as fumed silica and colloidal silica sol without the necessity to strictly control the synthesis conditions, being a convenient and reliable method for synthesis of Ti-rich TS-1 free of extraframework Ti species.

3.2. Crystallization Mechanism of TS-1 in the YNU System.

3.2.1. Crystallization Curves of TS-1 in the YNU and the Method A Systems. As mentioned above, in order to study the crystallization mechanism of zeolites, both the solid and liquid fractions in the system should be considered. Figure 4 shows the crystallinity of the TS-1 and silicalite-1 samples synthesized under different conditions in the YNU and method **A** systems (the Si/Ti ratio in the synthesis gel was 50 for both series of samples). It is clear that the presence of Ti in the gel not only severely retarded the crystallization process by prolonging the induction period but also reduced the crystallinity of most of the samples. Nevertheless, higher crystallinity of TS-1 was finally achieved in the YNU system than in the method **A** system.

In comparison to the sample crystallized in the method **A** system, TS-1 synthesized in the YNU system was more stable against hydrolysis under the crystallization conditions after the crystallization was completed. This may be due to the incorporation of more Ti cations into the framework associated with a reduction in defect sites, resulting in higher hydrophobicity. Lamberti and co-workers found that the intensity of the OH band due to internal defective Si−OH groups progressively decreased with increasing Ti amount incorporated in the framework.[9,35] This shows that the insertion of Ti into the lattice of TS-1 has a mineralizing effect, reducing the framework

(45) Millini, R.; Massara, E. P.; Perego, G.; Bellussi, G. *J. Catal.* **1992**, *137*, 497.
(46) Lamberti, C.; Bordiga, S.; Zecchina, A.; Carati, A.; Fitch, A. N.; Artioli, G.; Petrini, G.; Salvalaggio, M.; Marra, G. L. *J. Catal.* **1999**, *183*, 222.
(47) Biecher, L.; Sasaki, J. M.; Santos, C. O. P. *J. Appl. Crystallogr.* **2000**, *33*, 1189.
(48) Ricchiardi, G.; Damin, A.; Bordiga, S.; Lamberti, C.; Spanò, G.; Rivetti, F.; Zecchina, A. *J. Am. Chem. Soc.* **2001**, *123*, 11409.
(49) Boccuti, M. R.; Rao, K. M.; Zecchina, A.; Leofanti, G.; Petrini, G. *Stud. Surf. Sci. Catal.* **1989**, *48*, 133.
(50) Smirnov, K. S.; van de Graaf, B. *Microporous Mater.* **1996**, *7*, 133.
(51) Henry, P. F.; Weller, M. T.; Wilson, C. C. *J. Phys. Chem. B* **2001**, *105*, 7452.
(52) Marra, G. L.; Artioli, G.; Fitch, A. N.; Milanesio, M.; Lamberti, C. *Microporous Mesoporous Mater.* **2000**, *40*, 85.

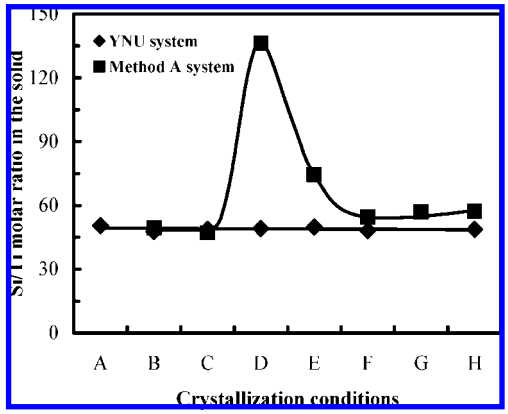

Figure 5. Dependence of the Si/Ti molar ratio of the solid fraction on the crystallization conditions in the YNU and method **A** systems. (A) 30 °C, 1 day; (B) 60 °C, 1 day; (C) 80 °C, 1 day; (D) 100 °C, 1 day; (E) 140 °C, 1 day; (F) 170 °C, 1 day; (G) 170 °C, 2 days; (H) 170 °C, 3 days.

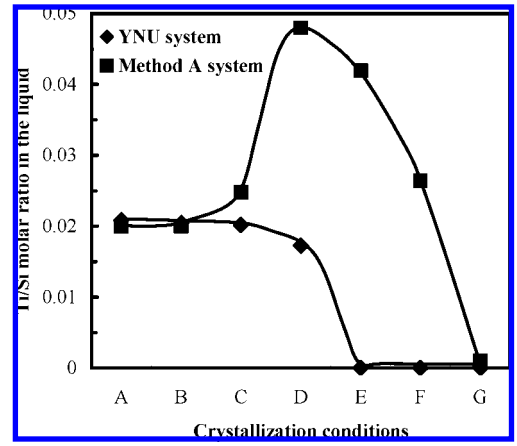

Figure 6. Evolution of the Ti/Si molar ratio in the liquid fraction during the whole crystallization process in the YNU and method **A** systems. (A) 30 °C, 1 day; (B) 60 °C, 1 day; (C) 80 °C, 1 day; (D) 100 °C, 1 day; (E) 140 °C, 1 day; (F) 170 °C, 1 day; (G) 170 °C, 3 days.

defects and, thus, increasing the hydrophobicity. This is also evidenced by the ^{1}H and ^{29}Si MAS NMR spectroscopic findings that silanol protons of H-bonded siloxy oxygens at defect sites proportionally decreased with the Ti atoms per unit cell.[53] In addition, the neutron diffraction study has revealed that among the 12 crystallographically independent T sites of the orthorhombic MFI framework, T_6, T_7, T_{10}, and T_{11} are the most possible sites for Ti to isomorphously substitute for Si, whereas the other sites could have low probability for Ti occupancy.[9,35] This is in good agreement with the Si vacancies in silicalite-1,[33] supporting the fact that the incorporation of more Ti atoms into the framework is accompanied by the parallel decrease in the defect sites.

An increase in the hydrophobicity by inserting Ti into the framework is further substantiated by the crystallization curves; the crystallinity of silicalite-1 decreased with increasing crystallization time after reaching the maximum. The presence of defect sites would make the material hydrophilic, causing an easy attack by once-adsorbed H_2O and, thus, a collapse of the framework (eq 1).

$$\equiv Si - O - Si \equiv + H_2O \rightarrow 2 \equiv Si - OH \qquad (1)$$

Figure 4 shows that the crystallization rate of TS-1 was much slower in the YNU system than that in the method **A** system. This is contrary to the result obtained by Kumar et al., who reported that the presence of oxyanions such as ClO_4^-, PO_4^{3-}, AsO_4^{3-}, and CO_3^{2-} ions in the synthesis system could significantly accelerate the crystallization of zeolites by speeding up the condensation process probably as a result of their great polarizing ability for the hydrophobic hydration balls, facilitating the nucleation of zeolites from the liquor.[54] This inconsistency may be due to the different crystallization mechanisms working in the Kumar's and the YNU synthesis systems. The crystallization in the former system occurred via a solution-mediated mechanism, whereas a solid-phase transformation mechanism seems to predominate in the latter synthesis system, which will be demonstrated in the following sections.

3.2.2. Evolution of the Chemical Compositions of the Solid Fraction and the Mother Liquid. Figure 5 shows the Si/Ti ratio of the solid samples collected in the whole crystallization process. The Si/Ti ratio in the solid samples synthesized in the YNU system was kept almost constant, being in the range of 48 and 50.5. This is similar to that found in the synthesis of TS-1 from amorphous wetness impregnated SiO_2-TiO_2 xerogels and the nonaqueous synthesis of zeolites with solid reaction mixtures where a solid-phase transformation mechanism predominated.[12,13] In addition, the solid yields recovered after calcination of all the YNU samples were always higher than 95% based on the added SiO_2 and TiO_2. This is also consistent with the occurrence of a solid-phase transformation mechanism. This would be favorable for the incorporation of Ti cations into the framework since dissociation, coalescence, and reorganization are the main processes during nucleation and crystal growth. In contrast, the Si/Ti ratio in the samples synthesized by method **A** drastically increased during the period of crystal growth; here the solid samples in the induction period were directly obtained by drying the liquid at 100 °C since no solid was formed during this period. This suggests that during the period of rapid crystal growth in the method **A** system, silicic and/or silicate species ($\equiv Si-OH$, $\equiv Si-O^-$) were polymerized with each other at a much higher rate than the condensation of silicic or silicate species and titanic or titanate ($\equiv Ti-OH$, $\equiv Ti-O^-$) species to form TS-1 crystals. The Ti content in the solid remarkably increased after the sample reached the highest crystallinity, indicating that most of Ti cations were incorporated into the framework after the crystallization was nearly completed. It was found that nuclei were formed from a clear solution in the method **A** system; the typical XRD pattern of the MFI structure was detected when the synthesis was carried out at 80 °C for 1 day, verifying that the nuclei have been formed and that the induction period has been completed, but at this stage the gel remained transparent. This shows that the crystallization in the method **A** system occurred via a homogeneous nucleation mechanism although precursor aggregates might be formed before nucleation, as reported by some researchers.[17–27] It can be also seen from Figure 5 that in this stage the Ti content in the as-synthesized YNU products was higher than in the **A** products, suggesting the incorporation of more Ti cations into the framework.

The evolution of the Ti/Si ratio in the mother liquid during the whole crystallization process (Figure 6) is in agreement with that of the solid samples. In the method **A** system, the Ti/Si ratio of the liquid phase sharply increased from the point after

(53) Parker, W. O.; Millini, R. *J. Am. Chem. Soc.* **2006**, *128*, 1450.
(54) Kumar, R.; Bhaumik, A.; Ahedi, R. K.; Ganapathy, S. *Nature* **1996**, *381*, 298.

the nuclei formed and reached the highest value when crystallization was almost completed. This shows that the majority of Ti species were still present in the liquid during the crystal growth period, while a large amount of silicic and silicate species and/or silicate polyanions have condensed with tiny amorphous precursor aggregates to form more nuclei or result in the growth of crystals. It seems that after the zeolitic architecture was almost built Ti cations started to be inserted into the framework. This suggests that Ti cations did not randomly substitute for Si but selectively occupied specific positions or defect sites, in accordance with the assumption made by other researchers and supported by the several types of spectroscopic and crystallographic data on both TS-1 and defective silicalite-1.[9,34,35,38,39,55] Here, it should be mentioned that although partially calcined nano-TS-1 (nanoscopic building units of TS-1) devoid of physisorbed TPAOH exhibited catalytic activity and selectivity in the oxidation of some organics,[56] it gave a conversion of about $^1/_{12}$ as low as that obtained over the conventional TS-1 in the competitive epoxidation of 1-hexene and cyclohexene (Table 2 in ref 56). However, if all the Ti cations were truly incorporated in the framework, calcined nano-TS-1 would show a higher activity than the conventional TS-1, particularly for the epoxidation of cyclohexene, due to the significant decrease in the steric constraint on the diffusion of substrates/products. The observed contrary results suggest that most of Ti cations were not incorporated in the framework, as confirmed by the absence of an IR band at 960 cm^{-1} after calcination of the sample at 550 °C.[56] The presence of a small number of tetrahedral Ti species in the nano-TS-1 would be possible, since the MFI nanostructure (double five-membered ring) has been formed. Therefore, the results obtained on the nano-TS-1 are not contradictory to our finding that most of Ti cations were inserted into the lattice after the crystallization was nearly completed.

In contrast, in the YNU system, the Ti/Si ratio in the liquid was almost constant (about 0.02) during the induction period, being the same as that in the solid fraction. After nuclei formed, a small amount of titanic and/or titanate species (more than 95% of silicon and titanium was kept in the solid fraction through the crystallization process) in the mother liquid quickly transferred into the solid, and the transfer rate was consistent with the crystal growth speed, as revealed by the ICP analyses (Figure 6) in combination with XRD results (Figure 4); the Ti content in the mother liquid decreased to 0 when the crystallization conditions were changed from 100 °C for 1 day (the formation of the MFI structure was just detected by XRD) to 140 °C for 1 day (the crystallization was nearly completed). This shows that the crystallization mechanism in the YNU system is completely different from that working in the method **A** system. Nevertheless, the decrease in the Ti/Si ratio in the liquid during the crystal growth period is indicative of the occurrence of a liquid-to-solid mass transfer of Ti as well as the solid-phase transformation which probably dominated the crystallization process. The complete depletion of Ti species in the liquid in the YNU system is in contrast to part of Ti species left in the liquid in the method **A** system, further evidencing that more Ti cations can be incorporated in the framework by the YNU method than by method **A**.

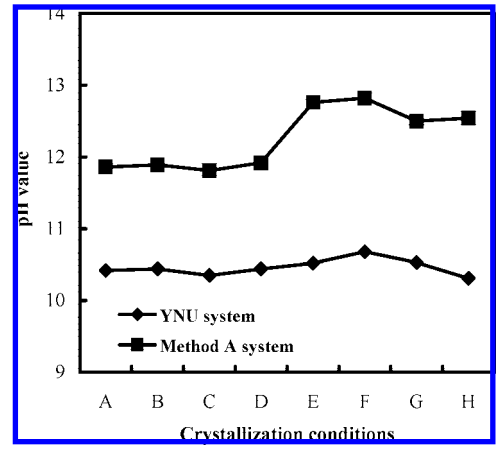

Figure 7. Evolution of the pH value of the liquid fraction during the whole crystallization process in the YNU and method **A** systems. (A) After addition of $(NH_4)_2CO_3$ for the YNU system; after removal of ethanol for the method **A** system. (B) 30 °C, 1 day; (C) 60 °C, 1 day; (D) 80 °C, 1 day; (E) 100 °C, 1 day; (F) 140 °C, 1 day; (G) 170 °C, 1 day; (H) 170 °C, 3 days.

3.2.3. Changes in the pH Value of the Mother Liquor during the Whole Crystallization Process. The relationship between the pH value of the mother liquor and the crystallization conditions is illustrated in Figure 7. After the addition of $(NH_4)_2CO_3$, the pH value of the liquid sample swiftly lowered from 11.9 to 10.4 and was thereafter unchanged during the induction period. In contrast, the pH value in the method **A** system remained 11.9 in the induction period. The hydroxide anion is an excellent mineralizer. As a ligand for Si^{4+} and Ti^{4+} ions, it allows the condensation of moderately stable silicic/silicate and titanic/titanate species to occur, resulting in the formation of zeolite species. The hydroxide ion concentration not only can alter the crystallization time for a particular structure but also could induce a change in the composition and sometimes the structure of the crystallized samples.[57]

In the synthesis of TS-1 in the method **A** system, the hydroxide ion of TPAOH plays a major role in accelerating the hydrolysis of the silica source and Ti alkoxide and the oligomerization of Si−OH and Ti−OH species (eq 2). These processes would lower down the pH value. Therefore, a high pH value could promote these processes and thus decrease the time for reaching the critical concentration of soluble silica and titanium species from which zeolites are ultimately precipitated. However, a very high alkaline condition would make the synthesis gel unreacted but dissolve the silicate/titanosilicate species (eq 3, from right to left), resulting in a lower crystallinity of the products crystallized in the method **A** system and the presence of more defect sites (Figure 4). In contrast, for the YNU system, the synthesis gel was quickly solidified after the addition of $(NH_4)_2CO_3$. Thus, most of TPA^+ species were embedded in the solid with the amount of free OH^- species drastically decreasing and with the pH value of the liquid lowering down. The lower the pH value, the higher the yield of crystalline material[57] or the more well-crystallized the product because the condensation reaction (eq 3, from left to right) proceeds to a greater extent. This accounts for the higher crystallinity of the TS-1 samples achieved by the YNU method than by method **A**.

(55) Marra, G. L.; Tozzalo, G.; Leofanti, G.; Padovan, M.; Petrini, G.; Genoni, F.; Venturelli, B.; Zecchina, A.; Bordiga, S.; Ricchiardi, G. *Stud. Surf. Sci. Catal.* **1994**, *84*, 559.

(56) Ravishankar, R.; Kirschhock, C.; Schoeman, B. J.; De Vos, D.; Grobet, P. J.; Jacobs, P. A.; Martens, J. A. In *Proceedings of the 12th International Zeolite Conference*; Treacy, M. M. J., Marcus, B. K., Bisher, M. E., Higgins, J. B., Eds.; Materials Research Society, 1999; p 1825.

(57) Szostak, R. *Molecular Sieves*, 2nd ed.; Blackie Academic & Professional, an imprint of Thomson Science, 1998; p 100.

$$x(\mathrm{TPA^+OH^-}) + \mathrm{T(OR)_4} + (4-x)\mathrm{H_2O} \rightleftharpoons ((\mathrm{TPA^+})_x(\mathrm{^-O})_x\text{-T})(\mathrm{OR})_{4-x}) + x\mathrm{ROH} + (4-x)\mathrm{H_2O} \rightleftharpoons (\mathrm{TPA^+})_x(\mathrm{^-O})_x\text{-T})(\mathrm{OH})_{4-x}) + (4-x)\mathrm{ROH} \quad (\mathrm{T = Si, Ti}) \quad (2)$$

$$\equiv\mathrm{Si-O^-} + \equiv\mathrm{TOH} \rightleftharpoons \equiv\mathrm{Si-O-T}\equiv + \mathrm{OH^-} \quad (\mathrm{T = Si, Ti}) \quad (3)$$

As expected, an increase in the pH value during the crystal growth period was observed for both synthesis systems, but the degree was much more appreciable for the method **A** system than for the YNU system. The pH value increased from 11.9 to 12.8 in the method **A** system, whereas it increased only slightly from 10.4 to 10.7 in the YNU system (Figure 7). The increase in the pH value is attributed to the incorporation of silicate species into the framework of TS-1, which releases free OH^- (eq 3). This increase continued till the completion of crystal growth. The higher OH^- concentration in the method **A** system also accelerates the crystal growth. Such a high crystallization rate is not beneficial for the incorporation of Ti into the framework since this process would make the local structure around Ti distorted. In addition, the high alkalinity of the liquid is unfavorable to the condensation of Ti−OH and silicate species. In contrast, the presence of $(NH_4)_2CO_3$ appropriately slows down the crystallization rate by significantly decreasing the pH value, buffering the synthesis gel, and introducing NH_4^+, which is a structure-breaking cation in water,[58] and consequently reducing the polymerization rate of silicic/silicate/titanic/titanate species. This would provide enough time for Ti species to be inserted into the lattice during the crystallization process, as indicated by the much lower Si/Ti ratio in the solid samples obtained during the crystal growth period in the YNU system than in the method **A** system. An optimum OH^- concentration could not only promote the crystallization of TS-1 and favor the incorporation of Ti into the framework but also inhibit the subsequent dissolution of the framework and/or the transformation to a more stable structure. It is not clear at this moment if there exists an interaction between TPA^+ cations and CO_3^{2-} anions, but this could not be excluded since the gel quickly solidified and the pH value significantly lowered down after addition of $(NH_4)_2CO_3$. Work on the effect of the counteranions of ammonium ion on the synthesis of TS-1 is in progress and will be reported in the near future.

3.2.4. Structure Formation Process and Ti Coordination States. Figure 8 shows the crystallite sizes and morphology of the samples synthesized in the YNU system under different crystallization conditions. It is clear that the initially formed particles had a flat and smooth surface with a size of about 5 μm (Figure 8A). With crystallization going on, the bulky gel particles gradually dissociated into aggregates of small pieces. This is the so-called secondary gel since no diffraction peaks characteristic of the MFI structure could be detected with XRD. This is in line with the findings, obtained by Dokter et al. through time-resolved small- and wide-angle X-ray scattering techniques, that an intermediate gel phase is required to start nucleation and crystallization.[17] When the sample was crystallized at 100 °C for 1 day, XRD measurement demonstrated the formation of nuclei although the particle morphology was basically unchanged; the XRD pattern typical of the MFI structure could be just discerned under these conditions (Figure 4D). The nuclei of TS-1 were very small and somewhat irregular in shape, rendering much difficulty in differentiating them from amorphous materials. Figure 8E suggests that nuclei might have evolved from the inner part of the particles, which is in agreement with the solid-phase transformation mechanism working in the YNU system.[13,14] It was recently proposed that high supersaturation within the gel particles possibly coupled with preorganization at the interface of the amorphous network with occluded solution could be the driving force for nucleation of zeolites, e.g., of zeolite A;[18] however, this is based on the assumption that the gel particle size is unchanged through the crystallization process. Obviously, this is not in line with the FE-SEM observations of the TS-1 samples synthesized in the YNU system. Thus, the occurrence of a solid-phase transformation mechanism would be more favorable in the YNU system. After nuclei formed, irregular crystals of sizes less than 200 nm progressively grew into spherical and further boat-shaped particles accompanied by depletion of the amorphous gel and restructuring (Figure 8F−I).

The formation of the secondary gel was also proved by TG measurement. The YNU samples collected in the induction period had four weight-loss regions (<100, 140−267 (or 110−263), 267−400, and 400−530 °C) (not shown here). The weight loss below 100 °C is due to the desorption of physically adsorbed water, whereas the weight losses in the last three regions are correlated with gelatinated water and templating molecules. The YNU sample synthesized at 60 °C for 1 day showed an increased weight loss between 110 and 263 °C, compared with the sample synthesized at 30 °C for 1 day. This is perhaps a result of the increase in hydrophilicity. This could be attributed to the dissociation and rearrangement/restructuring of the initial solid gel to form a secondary gel.[13,17]

It has been confirmed by $^1H-^{29}Si$ CP MAS NMR spectroscopy that in the synthesis of silicalite-1 by the same method as method **A** except that Ti was absent, short-range intermolecular interactions exist within van der Waals contact distance prior to the formation of nuclei, resulting in the formation of a preorganized inorganic−organic composite.[15,16] Kirschhock and co-workers also suggested that the formation of silicate polyanions with a curved hydrophobic SiO_2 surface by means of TPA^+ cations initiates the nucleation of silicalite-1.[22,23] The presence of a large quantity of organic template in the gel aggregates, where nuclei are formed, has been also found in the synthesis of zeolites A and Y.[18,19] Since the YNU samples were fully washed with distilled water before drying, and the dried gel was heavier than the materials added as sources of SiO_2, TiO_2, and TPAOH, it is believable that most of the added TPA molecules were primarily embedded in the solid after the addition of $(NH_4)_2CO_3$. This is also substantiated by the strong and broad exothermal peaks between 200 and 500 °C in the corresponding DTA curves (Supporting Information Figure S1, parts A−C). The formation of inorganic−organic composites in the YNU system provides the possibility for the nucleation in the solid fraction.

The three weight-loss regions between 140 and 530 °C observed for the YNU samples collected during the nucleation period indicate different local environments of templating molecules, as a consequence, showing broad exothermal peaks in the DTA curves. In the synthesis of MFI-type molecular sieves in the presence of TPAOH, it has been suggested that hydrophobic hydration balls are formed by H_2O molecules encircling TPA^+ cations with H_2O partially or completely substituted by silicate or aluminosilicate species.[15,16] This is

(58) Gabelica, Z.; Blom, N.; Derouane, E. G. *Appl. Catal.* **1983**, *5*, 227.

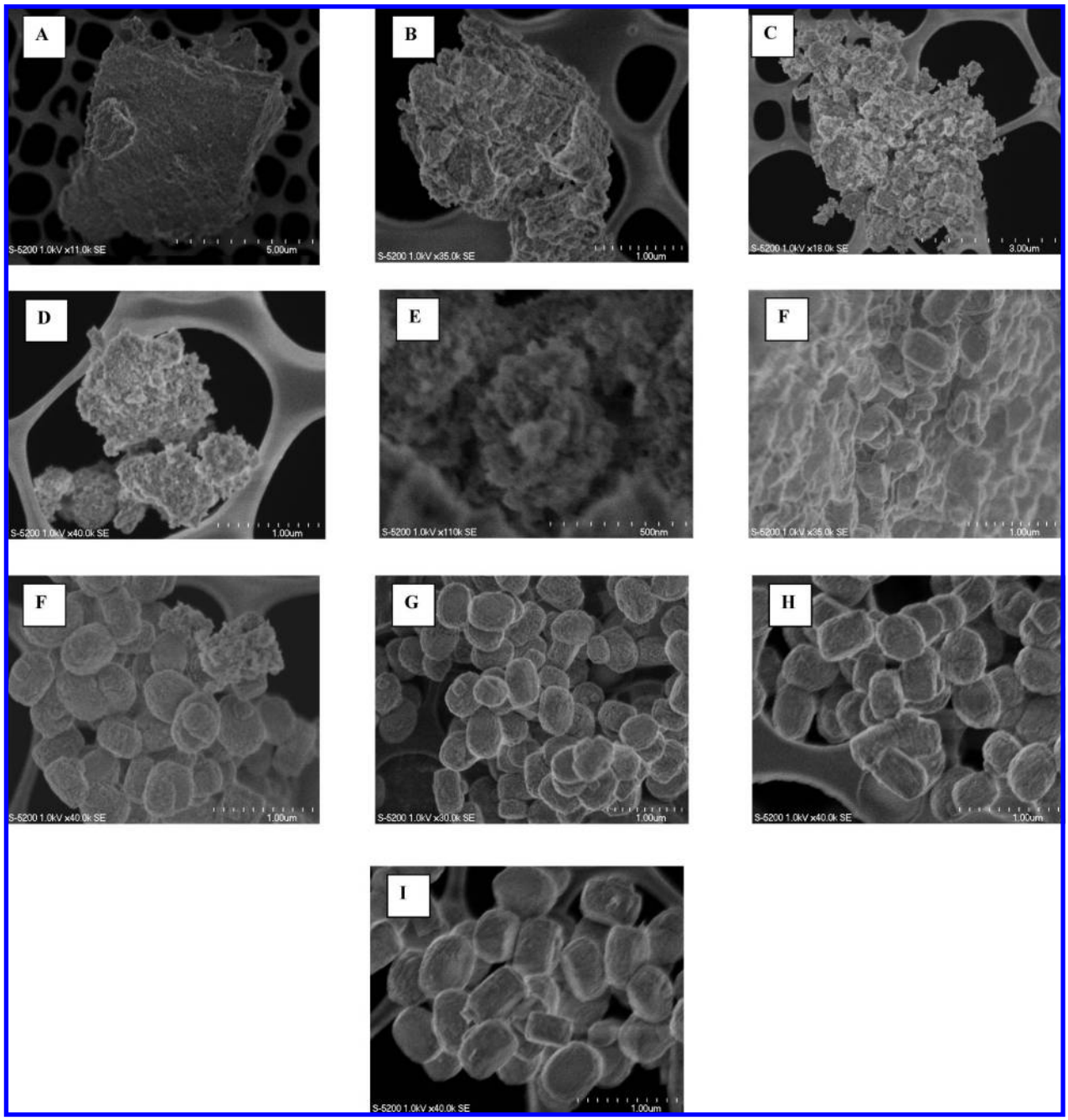

Figure 8. FE-SEM images of the solid samples collected under different crystallization conditions in the YNU system: (A) 30 °C, 1 day; (B) 60 °C, 1 day; (C) 80 °C, 1 day; (D) 100 °C, 1 day; (E) 110 °C, 1 day; (F) 120 °C, 1 day; (G) 140 °C, 1 day; (H) 170 °C, 1 day; (I) 170 °C, 3 days.

certainly applicable to the synthesis of TS-1 in the method **A** system since there is no essential difference with the exception that Ti species are present. Addition of $(NH_4)_2CO_3$ to the synthesis mixture led to an immediate solidification of the gel and, thus, the probable formation of hydrophobic hydration balls with different sizes and/or condensation degrees around TPA^+ by gelatinating the $Si(OH)_4$ and $Ti(OH)_4$ species with H_2O molecules followed by replacement of H_2O molecules with silicate and titanosilicate species. In addition, unlike in the method **A** system, in the YNU system the physical embedding of some TPAOH molecules could also be possible during the gelatination process. With the progress of crystallization, the inorganic−organic composite gel was restructured into zeolite nuclei, followed by the crystal growth at the expense of amorphous nutrients.

We concluded from the TG results that the unit-cell composition of the YNU sample crystallized at 170 °C for 3 days was $3.9TPA^+/96TO_2/2.9H_2O$. This is consistent with that of the ideal MFI-type structure where 4 TPA^+ cations were contained per 96 SiO_2 units. This verified that, in the as-synthesized TS-1 products, there was only one type of TPA^+ cation tightly enclathrated in the channel intersections. This is supported by the DTA measurement that showed only a very sharp exothermal peak at 385 °C with a shoulder around 430 °C for the well-crystallized product (Supporting Information Figure S1, part H).

As for the MFI-type molecular sieves, in addition to a structural band at 440−470 cm^{-1} (T−O bending mode), a typical band near 550 cm^{-1} should be observed in their

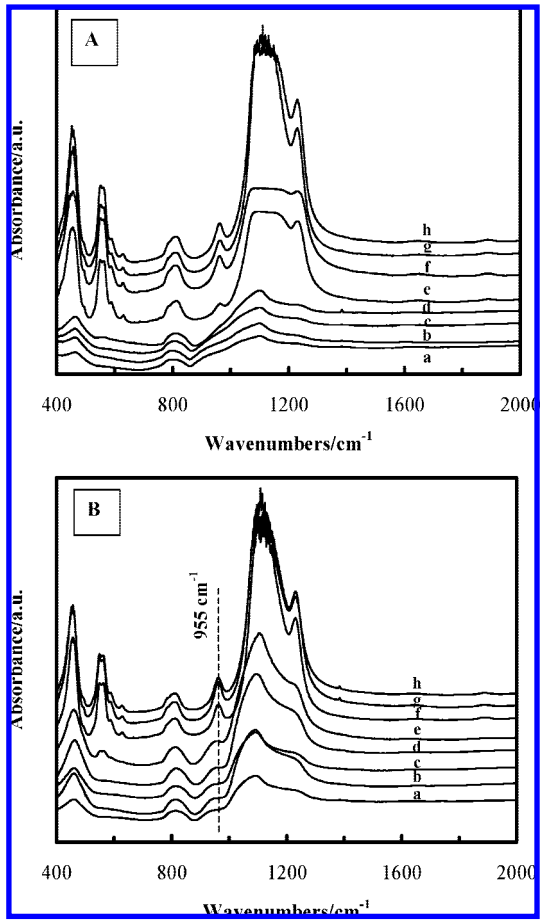

Figure 9. Framework IR spectra of the samples synthesized in the method **A** (A) and YNU (B) systems under different crystallization conditions: (a) after removal of ethanol (method **A** system) or after addition of $(NH_4)_2CO_3$ (YNU system); (b) 30 °C, 1 day; (c) 60 °C, 1 day; (d) 80 °C, 1 day; (e) 100 °C, 1 day; (f) 140 °C, 1 day; (g) 170 °C, 1 day; (h) 170 °C, 3 days.

framework IR spectra.[15,16,59,60] This is due to the stretching vibration of structural double five-membered rings.[15,16] The appearance of this band gives firm evidence that the sample possesses an atomic ordering of the MFI structure. In the method **A** system, the sample synthesized at 80 °C for 1 day showed a shoulder band around 550 cm^{-1} (curve d, Figure 9A). This is in agreement with the XRD finding that the peaks characteristic of the MFI structure already appeared (Figure 4) under these conditions, although the crystallinity was very low, viz., 2.8%. However, in the case of YNU samples, these XRD peaks could be detected only after the synthesis was conducted at 100 °C for 1 day and increased in intensity with increasing crystallinity (Figure 9B). These findings indicate that double five-membered rings or secondary structural units were formed from the clear solution in the method **A** system when the crystallization was carried out at 80 °C for 1 day; in contrast, they were formed in the YNU system when crystallization was continued at 100 °C for 1 day. This shows that the crystallization rate was slower in the YNU system, where the solid-phase transformation mechanism was operative, than in the method **A** system, where a homogeneous nucleation mechanism worked.

Nevertheless, both the **A** and YNU samples displayed a split of the band around 550 cm^{-1} into 549 and 559, and 546 and 559 cm^{-1}, respectively. This split was slightly less obvious for the **A** samples than for the YNU samples (Supporting Information Figure S2). This is in agreement with the findings for silicalite-1 nanophase material,[61] whereas there is a small difference in band positions. Although the basic reason is not clear, this is closely related to the sizes of particles containing five-membered rings, as reported by Kirschhock, Serrano, Hsu, and co-workers.[22,62–64] The precursor (2−3 nm) and nanoslabs ($1.3 \times 4 \times 4$ nm^3) of silicalite-1 exhibit the IR adsorption bands at 590−570 cm^{-1},[22,62,64] whereas colloidal particles with a size in the range of 18−100 nm, formed by extending the crystallization time, show a doublet at 555 and 570 cm^{-1}.[61] In contrast, micrometer-sized crystals display a band around 550 cm^{-1}.[15,16,22,59,60,62] This frequency shift also holds true for the TS-1 and the agglomeration of its nanoparticles by calcination,[56] suggesting that both the **A** and YNU samples might be composed of similar primary particles since both materials have the same IR adsorption band at 559 cm^{-1}. These primary particles are further aggregated into zeolite crystals, resulting in the shift to 546 and 549 cm^{-1} for YNU-50 and **A**-50, respectively. The slightly lower frequency of the former sample compared to the latter one might be due to the aggregation into larger particles.[22,56,61,62,64] This implies that zeolite crystals are possibly formed through a similar aggregation process irrespective of whether crystallization occurs via a solution-mediated mechanism or a solid-phase transformation mechanism.

Another important and distinctive feature of IR spectra of TS-1 is the band at about 960 cm^{-1}. Although the assignment of this band is still in debate,[35,48–50] the presence of this band after dehydration of samples under high-vacuum conditions is generally accepted as a solid proof for the incorporation of Ti into the framework. In agreement with previous results,[48] this band could not be observed in the IR spectra of the samples obtained in the induction period in the method **A** system (curves a−d in Figure 9A). When the crystallinity reached about 66% after further crystallization, this band was discernible. Then it sharply increased in intensity with the progress of crystallization. This is consistent with the marked increase in the Ti content in the solid and liquid fractions, verifying that Ti species were mainly inserted into the lattice in the method **A** system after the crystallization was nearly completed; no apparent increase in the intensity of the band at about 550 cm^{-1} was observed with the progress of crystallization after the sample was crystallized at 100 °C for 1 day.

In contrast, Figure 9B clearly shows a broad band around 955 cm^{-1} even just after the addition of $(NH_4)_2CO_3$ (curve a), and this band progressively increased in intensity with crystallization going on. This indicates that the Si−O−Ti groups were formed by gelatination from the beginning in the YNU system. With the solid gel structure dissociated and reorganized, more and more Si−OH and Ti−OH species were condensed to form Si−O−Ti groups, which then produced the secondary building units of TS-1 with precursor aggregates and/or with Si−O−Si and Si−OH species in the presence of TPA^+ cations, and the inorganic−organic composites were further gradually organized

(59) Jacobs, P. A.; Derouane, E. G.; Weitkamp, J. *J. Chem. Soc., Chem. Commun.* **1981**, 591.
(60) Coudrier, G.; Naccache, C.; Vedrine, J. C. *J. Chem. Soc., Chem. Commun.* **1982**, 1413.
(61) Ravishankar, R.; Kirschhock, C.; Schoeman, B. J.; Vanoppen, P.; Grobet, P. J.; Storck, S.; Maier, W. F.; Martens, J. A.; De Schryver, F. C.; Jacobs, P. A. *J. Phys. Chem. B* **1998**, *102*, 2633.
(62) Kirschhock, C. E. A.; Ravishankar, R.; Verspeurt, F.; Grobet, P. J.; Jacobs, P. A.; Martens, J. A. *J. Phys. Chem. B* **2002**, *106*, 3333.
(63) Serrano, D. P.; van Grieken, R. *J. Mater. Chem.* **2001**, *11*, 2391.
(64) Hsu, C. Y.; Chiang, A. S. T.; Selvin, R.; Thompson, R. W. *J. Phys. Chem. B* **2005**, *109*, 18804.

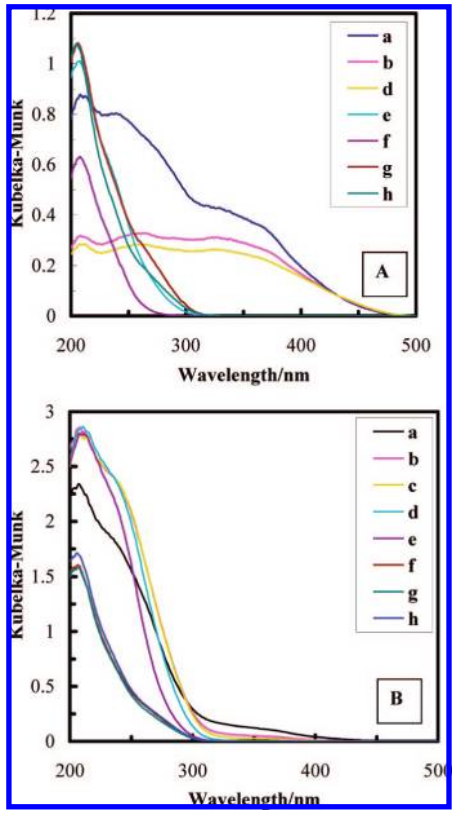

Figure 10. DR UV−vis spectra of the as-synthesized solid samples obtained under different conditions: (a) after removal of ethanol (method **A** system) or after addition of $(NH_4)_2CO_3$ (YNU system); (b) 30 °C, 1 day; (c) 60 °C, 1 day; (d) 80 °C, 1 day; (e) 100 °C, 1 day; (f) 140 °C, 1 day; (g) 170 °C, 1 day; (h) 170 °C, 3 days in the method **A** (A) and YNU (B) systems, respectively.

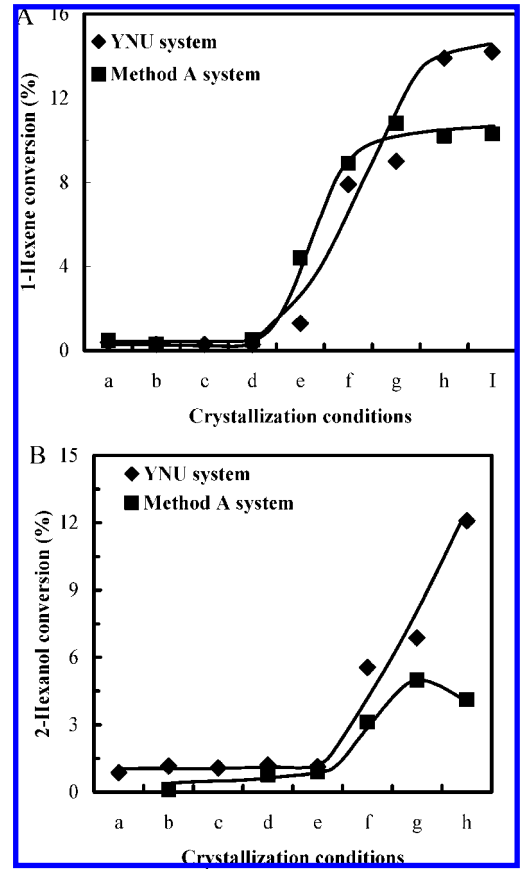

Figure 11. Catalytic properties of the **A** and YNU samples collected in different crystallization conditions for (A) the oxidation of 1-hexene (a) after removal of ethanol (method **A** system) or after addition of $(NH_4)_2CO_3$ (YNU system); (b) 30 °C, 1 day; (c) 60 °C, 1 day; (d) 80 °C, 1 day; (e) 100 °C, 1 day; (f) 140 °C, 1 day; (g) 170 °C, 1 day; (h) 170 °C, 3 days; (I) 170 °C, 5 days and for (B) the oxidation of 2-hexanol (a) after removal of ethanol (method **A** system) or after addition of $(NH_4)_2CO_3$ (YNU system); (b) 30 °C, 1 days; (c) 60 °C, 1 day; (d) 80 °C, 1 day; (e) 100 °C, 1 day; (f) 140 °C, 1 day; (g) 170 °C, 1 day; (h) 170 °C, 3 days. (Reaction conditions: 0.05 g of catalyst, 10 mL of methanol, 10 mmol of substrate, 10 mmol of H_2O_2, 60 °C, 2 h.)

into the MFI architecture. This further confirms that the insertion of Ti into the framework started from the early nucleation period in the YNU system and coincided well with the crystallization process of the MFI structure. As a result, the incorporation of more Ti cations into the lattice was attained.

The Ti coordination state during the whole crystallization process was further investigated with DR UV−vis spectroscopy. Both the as-synthesized YNU and **A** samples collected in the induction period contained three types of Ti species, i.e., tetrahedral, octahedral, and tiny Ti oxide particles (Figure 10). Nevertheless, many more tetrahedral Ti species were present in the YNU samples, whereas the **A** samples collected at the early crystallization period contained many more Ti oxides, as evidenced by the presence of an intense band around 330 nm in their DR UV−vis spectra. This is indicative of the presence of a large number of isolated $Ti(OH)_4$ species in the crystalline gel of the method **A** system during the nucleation period. Even after calcination and the following acid treatment, more octahedral Ti species were still present in the **A** samples than in the YNU samples since a more intense band at about 260 nm was observed for the **A** samples despite the disappearance of the tiny Ti oxide particles (Supporting Information Figure S3). This implies that the condensation degree of Si−OH and Ti−OH species in the method **A** system was much lower than in the YNU system during the nucleation period; all the samples were dried at 100 °C and washed with acid under the same conditions. In addition, the coordination state of Ti species in the **A** samples obtained in the induction period was basically unchanged with the progress of crystallization, giving another piece of evidence for the predominant incorporation of Ti into the framework after zeolitic architecture was nearly built. In contrast, more and more Ti cations were transformed from octahedral coordination species into tetrahedral-to-octahedral and tetrahedral ones in the YNU system, as revealed by the gradual shift to the lower-wavelength positions and the decrease in the intensity of the bands ascribed to octahedral Ti species and Ti oxides with increasing crystallization degree. This further proves that substitution of Ti for Si concomitantly occurred with nucleation in the YNU system.

3.2.5. Catalytic Performance of the Solid Samples Collected under Different Conditions. Ti-containing solid samples synthesized under different conditions in the method **A** and YNU systems were further examined for the oxidation of 1-hexene and 2-hexanol (Figure 11). Herein, all the samples were calcined and successively treated with hydrochloric acid (0.5 mol L^{-1}, liquid/solid = 50 mL g^{-1}) at room temperature for 24 h. Clearly, regardless of the synthesis systems, the amorphous samples obtained in the induction period showed a very low activity for the oxidation of both 1-hexene and 2-hexanol although some Ti cations have a tetrahedral coordination. After the formation of nuclei, the activity sharply increased with increasing crystallinity for both series of samples. TS-1 catalysts prepared from

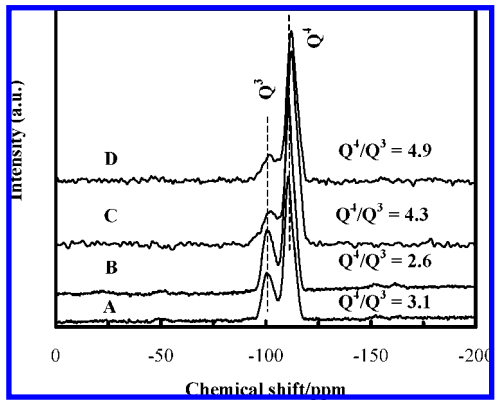

Figure 12. ^{29}Si MAS NMR spectra of the silicalite-1 and TS-1 samples synthesized in the method **A** system under different conditions: (A) silicalite-1, 170 °C, 1 day; (B) silicalite-1, 170 °C, 3 days; (C) TS-1, 170 °C, 1 day; (D) TS-1, 170 °C, 3 days.

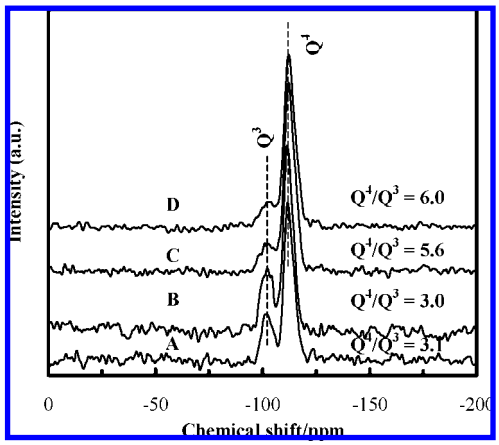

Figure 13. ^{29}Si MAS NMR spectra of the silicalite-1 and TS-1 samples synthesized in the YNU system under different conditions: (A) silicalite-1, 170 °C, 1 day; (B) silicalite-1, 170 °C, 3 days; (C) TS-1, 170 °C, 1 day; (D) TS-1, 170 °C, 3 days.

the YNU system showed significantly higher conversion than the samples prepared from the method **A** system partly as a result of the incorporation of more Ti species into the framework. This also holds true for the oxidation of 2-hexanol. It is worth noting that the highest conversion for the oxidation of 1-hexene and 2-hexanol over the **A** samples was achieved when crystallization was carried out at 170 °C for 1 day. In contrast, with respect to the YNU samples, the activity in the oxidation of 2-hexanol significantly increased when the crystallization time at 170 °C was elongated from 1 to 3 days although the two samples had similar crystallinities.

Figure 6 shows that in the method **A** system, Ti cations continued to transfer from the liquid into the solid after the sample was crystallized at 170 °C for 1 day. However, 1-hexene and 2-hexanol conversions were not increased. This may result from the partial tethering and/or absorption of these Ti species on the solid, which can be easily removed by acid washing, as indicated by similar Ti contents in the prepared catalysts (Figure 5). This is probably because most of the Ti cations have already been inserted into the preferable lattice sites at this stage, and thus, the rest of the sites would be much more difficult to be replaced with Ti. However, this is not true for the YNU system. As shown in Figures 5, 6, and 9, all Ti species entered into the solid to achieve a tetrahedral coordination state when the crystallization was carried out at 140 °C for 1 day. The further

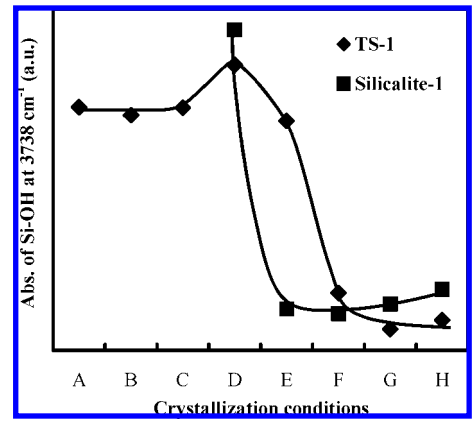

Figure 14. Dependence of the isolated Si−OH absorbance at 3738 cm^{-1} for the samples synthesized in the YNU system on the crystallization conditions: (A) after addition of $(NH_4)_2CO_3$; (B) 30 °C, 1 day; (C) 60 °C, 1 day; (D) 80 °C, 1 day; (E) 100 °C, 1 day; (F) 140 °C, 1 day; (G) 170 °C, 1 day; (H) 170 °C, 3 days.

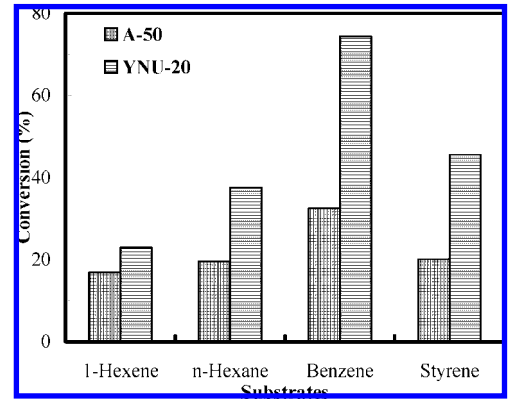

Figure 15. Catalytic results of the oxidation of various organic substrates over the YNU-20 and **A**-50 catalysts (H_2O_2 based conversion (%): the percent used for the oxidation of substrates. Reaction conditions: for 1-hexene, 0.05 g of catalyst, 10 mL of methanol, 10 mmol of substrate, 10 mmol of H_2O_2, 60 °C, 2 h; for *n*-hexane, 0.1 g of catalyst, 10 mL of methanol, 10 mmol of substrate, 20 mmol of H_2O_2, 60 °C, 4 h; for benzene, 0.1 g of catalyst, 10 mL of sulfolane, 10 mmol of substrate, 1 mmol of H_2O_2, 100 °C, 2 h; for styrene, 0.1 g of catalyst, 10 mL of acetone, 5 mmol of substrate, 2.5 mmol of H_2O_2, 60 °C, 4 h).

increase in the activity might be due to a slight improvement in microscopic Ti character stemming from further condensation of Ti species into Si−O−Ti groups and the resultant increase in hydrophobicity and slight change of the bond angle and the bond length of Si−O−Ti groups.

3.2.6. Location of Ti Cations in the Samples. It was reported that in the method **A** system Ti was preferably inserted into the defect sites.[9,34,35,38,39,55] This is supported by our experimental data showing that the isomorphous substitution of Ti for Si occurred mainly when crystal growth was almost completed and that TS-1 has a much smaller number of defect sites than silicalite-1 synthesized under the same conditions, as proved by the low intensity of the IR vibration band at 3738 cm^{-1} (not shown here), which is characteristic of isolated Si−OH groups. This is further confirmed by ^{29}Si MAS NMR spectroscopy; the signal at about 103 ppm of the TS-1 sample is considerably weaker in intensity than that of the silicalite-1 sample (Figure 12), which is solely attributed to Q^3 species ($(SiO)_3SiOH$) since the signal assigned to the ($(SiO)_3SiOTi$) species would appear at a higher field than Q^4 species ($(SiO)_4Si$) for the TS-1

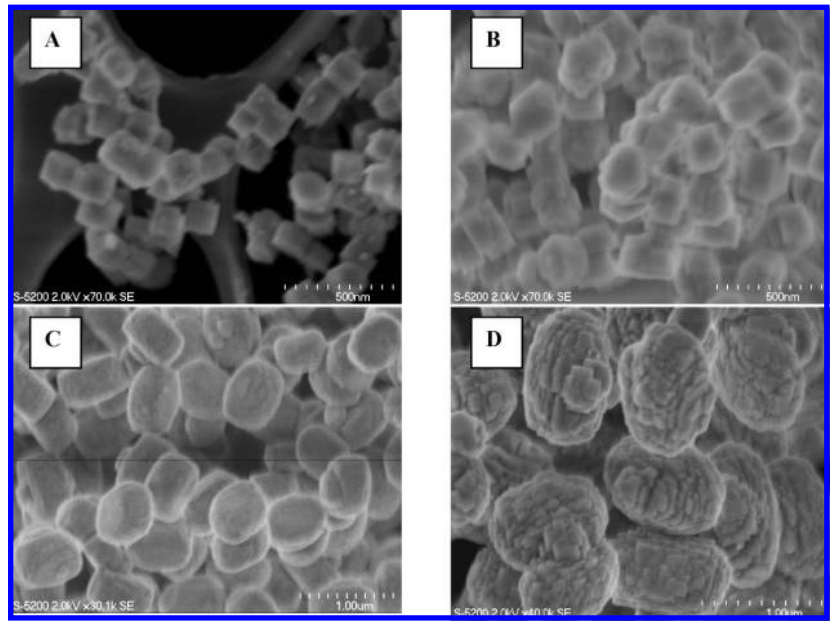

Figure 16. FE-SEM images of the **A**-50 (A), **A**-20 (B), YNU-50 (C), and YNU-20 (D) samples.

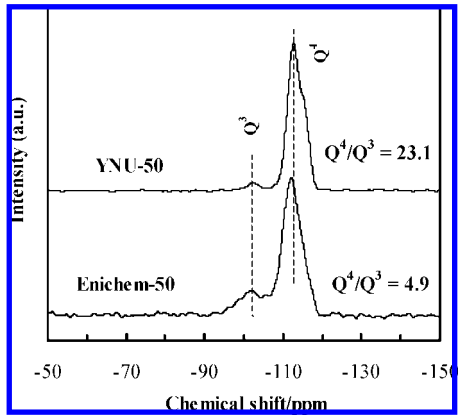

Figure 17. ^{29}Si MAS NMR spectra of the prepared TS-1 catalysts (the Si/Ti ratios are 58.3 and 57.2 for the **A**-50 and YNU-50 samples, respectively).

material.[65] The Q^4/Q^3 ratio of the silicalite-1 sample crystallized at 170 °C for 1 day was 3.1 in contrast to the ratio of 4.3 for the TS-1 synthesized under the same conditions. This is in agreement with the finding made by neutron powder diffraction study that Ti is not randomly distributed in the framework but preferably occupies some sites such as T_6, T_7, T_{10}, and T_{11}.[9,35] The silicalite-1 sample crystallized at 170 °C for 3 days showed a lower Q^4/Q^3 ratio than the sample crystallized for 1 day, indicating the presence of more defect sites in the former sample. This is consistent with the fact that the crystallinity of silicalite-1 decreased when the synthesis time was extended from 1 to 3 days (Figure 4, parts F and G), which is probably due to partial dissolution of the formed crystals upon further crystallization.

The presence of a smaller number of defect sites in the well-crystallized TS-1 than in the silicalite-1 also holds true for the YNU samples (Figure 13). Furthermore, it is worth noting that the Ti-containing solids obtained during the induction period in the YNU system contained less defect sites than pure silica solid analogues (Figure 14D). This is probably due to the formation of more Si−O−Ti and Si−O−Si groups in the former samples. Otherwise, the much higher crystallization rate in the silicalite-1 system (Figure 4D) would contrarily result in a higher condensation degree and, thus, the presence of a smaller amount of defect sites for the silicalite-1 sample synthesized at 100 °C for 1 day; under these conditions the crystallinity of silicalite-1 reached about 80%, whereas that of the YNU sample was less than 3%. This would lead to a more homogeneous distribution of Ti in the YNU samples than in the **A** samples because this creates the conditions for Si−O−Si and Si−O−Ti groups simultaneously to form a nucleus around TPA^+ cations and further build into a zeolitic architecture. In particular, it is noteworthy that all Ti species have been incorporated into the solid when the crystallinity reached the maximum. In contrast, in the method **A** system, almost all Ti cations were inserted into the defect lattice sites after crystallization was nearly completed. This is supported by the XPS data; the surface Si/Ti ratio in the calcined and subsequently acid-treated **A** samples gradually decreased with the progress of crystallization after reaching the highest crystallinity, whereas for the YNU samples it was basically unchanged (not shown here). Nevertheless, this cannot exclude the possibility that Ti prefers to replace Si in some certain lattice sites, e.g., defect sites in silicalite-1, for the YNU samples since TS-1 synthesized in the YNU system also shows a Q^3 signal much lower in intensity than silicalite-1 synthesized under the same conditions. An increase in the intensity of the isolated Si−OH vibration band before the formation of nuclei (Figure 14, parts C and D) is in accordance with the TG and FE-SEM findings that original bulky gel particles are first dissociated into aggregates of small pieces, viz., secondary gel, and then reorganized into zeolitic framework.

3.3. Catalytic Properties of Ti-Rich TS-1 Prepared from the YNU System. Table 1 shows the catalytic results of TS-1 prepared by the methods **A**, **B**, and YNU for the oxidation of *n*-hexane. For each series of catalysts, their catalytic properties were highly dependent on the framework Ti amount. Obviously, YNU samples gave much higher *n*-hexane conversion and ketone selectivity than either **A** or **B** (synthesized by method **B**) samples, and the difference was more apparent in the

(65) Tuel, A.; Ben Taarit, Y. *J. Chem. Soc., Chem. Commun.* **1992**, 1578.

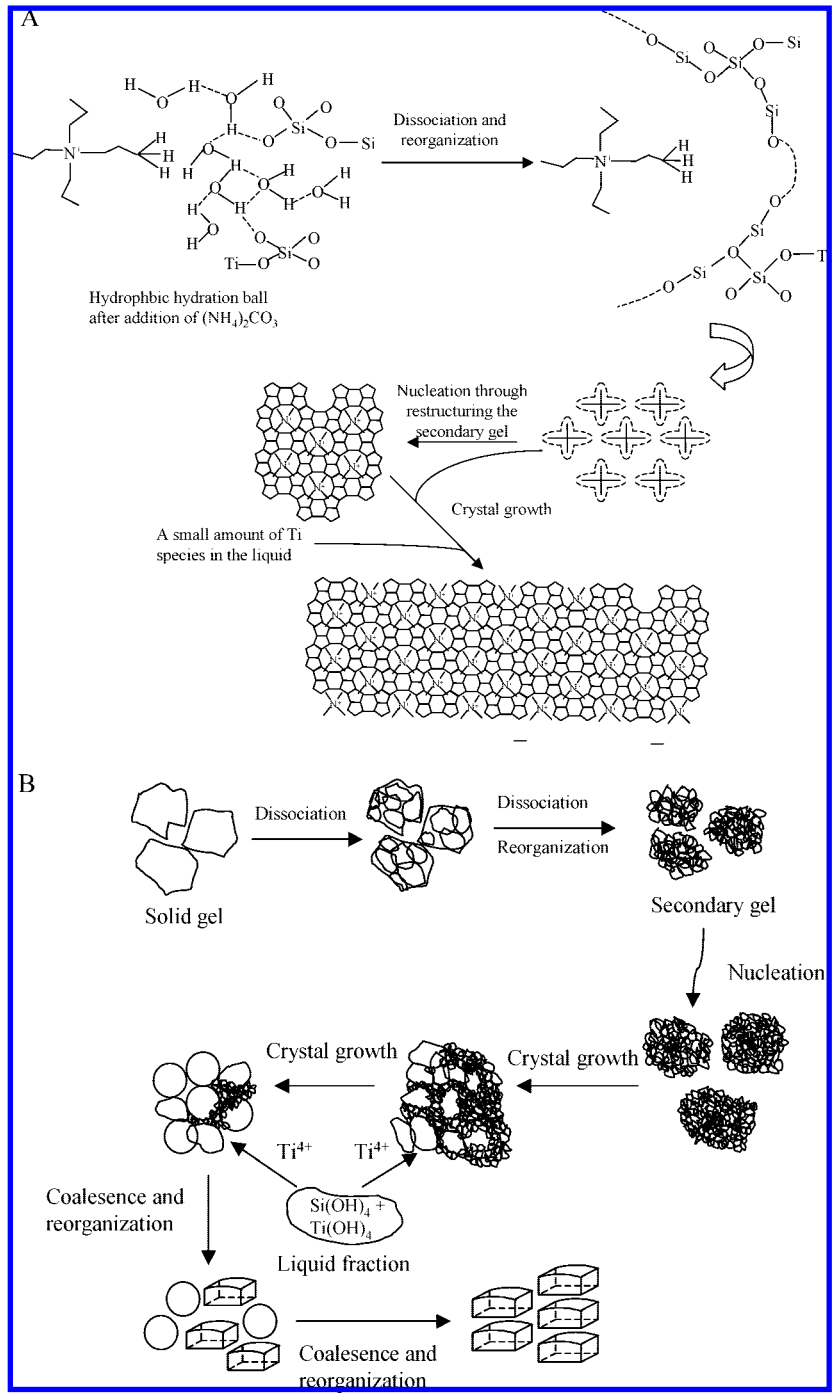

Figure 18. Schemes for the crystallization process: (A) the proposed mechanism for the formation of TS-1 and (B) the evolution of solid particle morphology occurring in the YNU system.

oxidation of other linear alkanes. The conversions based on H_2O_2 over the YNU-15 sample were 14.2%, 16.3%, and 10.7%, whereas they were 4.9%, 7.6%, and 3.7% on the **A**-50 sample in the oxidation of *n*-pentane, *n*-heptane, and *n*-octane, respectively, under the same reaction conditions. For comparison, Figure 15 shows the catalytic results of the oxidation of various organic substrates over the two best samples of **A**-50 and YNU-20 obtained by the methods **A** and YNU, respectively. It is clear that YNU-20 exhibited significantly higher catalytic activity than **A**-50 in the oxidation of not only alkanes but also other organic substrates such as 1-hexene, styrene, and benzene. This is attributable to both the higher Ti content in the YNU samples and the higher oxidation ability of Ti sites. YNU-20 gave turnover numbers (TONs) of 100, 160, 16, and 24 in contrast to 119, 140, 11, and 18 given by **A**-50 in the oxidation of 1-hexene, *n*-hexane, benzene, and styrene, respectively.

The oxidation ability of titanosilicates is correlated to the size of crystals, and the small crystals usually exhibit high reactivity. However, addition of $(NH_4)_2CO_3$ to the synthesis gel resulted in the formation of large crystals. FE-SEM measurements showed that the uniform crystal size of the YNU-50 sample was about 0.7 μm, being about 3.5 times as large as that of the **A**-50 sample (Figure 16). The morphology and crystal sizes of the **B** samples (not shown here) were similar to those of the **A** samples. The crystal sizes of the YNU samples further increased to larger than 1 μm with increasing Ti content for the YNU-

20. This is in accordance with the results reported by Cundy et al. that incorporation of more Ti into the framework resulted in the formation of larger crystals.[66] In contrast, no marked change in the crystal size was observed for the **A** and **B** samples when the Si/Ti ratio in the gel was increased. The fact that the crystal size of YNU samples was larger than of **A** samples is also consistent with the framework IR spectra, where the band assigned to the stretching vibration of double five-membered rings appeared at a lower frequency for YNU-50 than for **A**-50 (546 vs 549 cm^{-1}) (Supporting Information Figure S2).

One might consider that the increase in crystallite size would lead to low oxidation efficiency. However, in the case of YNU samples, crystals are well crystalline, as evidenced by higher Q^4/Q^3 ratio (Figure 17). In contrast, more defective sites were present in the **A** samples. This is consistent with the finding that the silanol groups or the defect sites decreased with increasing Ti content in the framework,[35,53] since Ti has a mineralizing effect and more Ti cations were incorporated in the YNU samples than in the **A** samples. Therefore, in comparison with the YNU samples, the **A** samples are not only relatively hydrophilic but might contain more ($(SiO)_3TiOH$) species. The higher hydrophilicity of the **A** samples than of the YNU samples is further corroborated by the fact that the weight loss below 150 °C due to the desorption of water was about 1.0% for as-synthesized **A**-50 in contrast to 0.3% for as-synthesized YNU-50 (not shown here).

Although the catalytic properties of titanosilicates are probably related to their crystalline structures and/or characters, the presence of more defect sites in titanosilicates would be unfavorable for the oxidation of alkanes, styrene, and benzene, as suggested by the following facts: (i) compared with TS-1, Ti-MWW, and Ti-Beta with more defect sites showed very low activity for the oxidation of *n*-hexane, styrene, and benzene; (ii) Ti-MCM-41, with a low Q^4/Q^3 ratio, showed very low activity in the oxidation of *n*-hexane and 1-hexene; however, silylation resulted in a remarkable improvement in the oxidation activity.[67] Furthermore, it has been proven that ($(SiO)_3TiOH$) species are much less active than ($(SiO)_4Ti$) species for the liquid-phase oxidation of organics over TS-1.[68,69] Therefore, although YNU samples have larger crystals, they showed higher catalytic efficiency. On the other hand, the finding that the TON of YNU samples increased with increasing Ti content up to the Si/Ti ratio of 57.2 can be accounted for by the decrease in the defect sites (Table 1). The fact that a further increase in the Ti content resulted in a slight decrease in the TON is probably due to the nonrandom distribution of Ti in the framework,[9,34,35,38,39,55] which would lead to the inclusion of some Ti cations in the lattice sites hardly accessible to substrate molecules.

4. Conclusions

A Ti-rich TS-1 sample has been synthesized by using $(NH_4)_2CO_3$ as a crystallization-mediating agent. The Si/Ti ratio in the framework can be decreased to 34 in contrast to 58 achieved by methods **A** or **B** under the same crystallization conditions. The prepared catalyst showed much higher activity than the **A** sample in the oxidation of a variety of organic substrates, e.g., linear alkenes and alkanes, alcohols, styrene, as well as benzene. This not only is due to the higher Ti content in the framework but also results from the increase in hydrophobicity.

Addition of $(NH_4)_2CO_3$ to the synthesis gel drastically lowered down the pH value to result in a slow crystallization rate, thus making the speed for the incorporation of Ti into the framework and the crystallization rate match well. Its addition also considerably modified the crystallization mechanism. In comparison to the typical liquid-phase transformation mechanism working in the method **A** system, solid-phase transformation mechanism seems to predominate in the YNU system although the simultaneous occurrence of a liquid-to-solid mass transfer after the formation of nuclei cannot be excluded. An overview of the crystallization process in the YNU system is illustrated in Figure 18 (scheme I for the proposed formation mechanism and scheme II for the evolution of particle morphology).

After the addition of $(NH_4)_2CO_3$, the clear solution quickly solidified to form an inorganic−organic gel composed of bulky particles, which were further depolymerized and reorganized into aggregates of tiny particles (secondary gel). Nucleation seems to start from the inner portion of the aggregates, followed by a crystal growth by depleting the nutrients in amorphous materials. The secondary gel particles first restructured into zeolite nuclei and then grew into irregular objects less than 200 nm in size. This was followed by the formation of a spherical shape and finally a boat habit.

During the induction period, no evidence was found for the mass transfer from liquid to solid or vice versa in the YNU system. This suggests that nuclei formed through dissociation and restructuring of the solid gel, and incorporation of Ti into the framework started from the gelatination process with the assistance of $(NH_4)_2CO_3$ in contrast to the method **A** system where most of Ti species were inserted into the lattice after the crystallization was nearly completed. With increasing crystallinity, a small part of nongelatinated Ti−OH species (and hence left in the liquid) quickly transferred into the solid. Although the crystallinity reached the highest value when crystallization was carried out at 140 °C for 1 day, the condensation of Ti−OH and Si−OH groups was still going on in the YNU system. Therefore, a further crystallization led to not only an increase in the hydrophobicity but also an overall improvement in the microscopic character of Ti species. As a result, the samples showed increased activity with the progress of crystallization after the zeolitic architecture was built.

Acknowledgment. The authors gratefully thank the Core Research for Evolutional Science and Technology of the Japan Science and Technology Agency (JST) for support of this work. W.F. also thanks JST for a postdoctoral fellowship and the Chinese Academy of Sciences ("Hundred Talents" Project) and the National Science Foundation of China (No. 20773153) for support of this work.

Supporting Information Available: DTA results of the YNU samples crystallized under different conditions, framework IR spectra of the **A**-50 and YNU-50 catalysts, DR UV−vis spectra of the calcined and further acid-treated solid samples synthesized in the method **A** and YNU systems under different conditions, Figures S1−S3. This material is available free of charge via the Internet at http://pubs.acs.org.

JA7100399

(66) Cundy, C. S.; Forrest, J. O.; Plaisted, R. J. *Microporous Mesoporous Mater.* **2003**, *66*, 143.
(67) Tatsumi, T.; Koyano, K. A.; Igarashi, N. *Chem. Commun.* **1998**, 325.
(68) Srinivas, D.; Manikandan, P.; Laha, S. C.; Kumar, R.; Ratnasamy, P. *J. Catal.* **2003**, *217*, 160.
(69) Zhuang, J.; Ma, D.; Yan, Z.; Deng, F.; Liu, X.; Han, X.; Bao, X.; Guo, X.; Wang, X. *J. Catal.* **2004**, *221*, 670.